Open Access Journal

Journal of Power Technologies 96 (3) (2016) 183–193

journal homepage:papers.itc.pw.edu.pl

Optimal reconfiguration and scheduling of a smart distribution network with uncertain renewables and price-responsive demand

Ahmad Ghasemi*

Department of Electrical and Computer Engineering, Jundi-Shapur University of Technology, Dezful, Iran

Abstract

A new two-stage operation scheduling framework is proposed in this paper to optimize day-ahead (DA) operation of a reconfigurable smart distribution network (SDN). The SDN contains wind farm as uncertain renewable generation as well as responsive demand and is operated by a distribution company (DisCo). The DisCo implements nodal hourly pricing as a price-based demand response program (DRP) to modify consumers' demand profile. Retail prices are determined in the first stage of the proposed scheduling framework, while the best network topology and the bidding strategy of the DisCo in the DA energy market are determined in the second stage. The two point estimate method (TPEM) is implemented in this paper to model the intrinsic uncertainty of wind farm power generation and responsive demand. Finally, the effectiveness of the proposed framework is evaluated in several case studies.

Keywords: Reconfiguration, Smart distribution network (SDN), Demand response, Retail pricing, Wind power generation, Uncertainty

1. Introduction

1.1. Aim

Distribution network reconfiguration has recently attracted a great deal of attention among power system researchers. Power system operators may also find it necessary to consider different possible configurations in operation scheduling optimization of distribution networks. However, network topology reconfiguration needs sophisticated communication and control infrastructures. Owing to advancements in Smart Grid (SG) systems, future distribution networks will be characterized by information and communication technology (ICT) [14]. Moreover, these smart distribution networks (SDNs) are equipped with advanced control infrastructures, like remotely controlled switches (RCSs), to attain flexible network topologies. On the other hand, benefiting from SG technologies, DisCos as SDN operators see an opportunity to implement the latest demand response programs (DRPs) based on optimal retail electricity pricing [17, 8]. The aim of this paper is to study the effect of network topology reconfiguration on day-ahead (DA) operation scheduling of a SDN with variable renewable generation and responsive demand.

*Corresponding author

Email address: raghasemi@jsu.ac.ir (Ahmad Ghasemi)

1.2. Literature Review

DA operation scheduling of a reconfigurable distribution network in the presence of renewable energy resources (RES) and responsive demand has been the focus of much recent research [11, 13, 20, 10]. In Ref. [5] the reconfiguration problem in the presence of distributed wind power generations has been studied. Microgrid load dispatch and network reconfiguration problems were solved together in Ref. [15]. In Ref. [12], a probabilistic network reconfiguration model was proposed to find the best configuration for each season, considering load and renewable generation uncertainty. The best topology for each hour was determined in Ref. [9] with the aim of minimizing power loss and switching cost. Responsive loads were also considered in this paper as an energy management option to reduce the operation cost [9]. In Ref. [10] a stochastic model was presented to optimize DA operation of a reconfigurable microgrid with wind turbines and dispatchable loads. Most studies in the context of distribution network operation benefiting from topology reconfiguration such as Refs. [13, 10, 9] have addressed the application of some initial DRPs, such as demand limiting and demand shedding. However, recent advancements in SG technologies means more sophisticated DRPs can be implemented through innovative retail pricing mechanisms. The concept of spot pricing of electricity was developed in Ref. [18]. A comprehensive demand response model based on price elasticity of demand was derived in Ref. [4]. In Ref. [6] optimal retail prices were determined based on the responsive load model developed in Ref. [4] to maximize the profit of an electricity retailer. The impact of optimal hourly pricing mechanism on energy acquisition of a DisCo was studied in Ref. [17]. In Ref. [8] a new DRP, i.e. hourly electricity pricing based on the location of load, was introduced by the authors. In the proposed DRP scheme, the location of load and price elasticity of demand, played the key roles in determining retail electricity prices for different consumers who participated in the program [8]. However, network topology was supposed to remain unchanged during the optimization period [8]. This may be an oversimplification in the actual power system operation and reduces the accuracy of the proposed pricing scheme. Topology reconfiguration capability may increase the efficiency of the proposed DRP scheme, especially in an environment embedded with uncertain renewable generation. In addition, the uncertainties associated with renewable power generation and responsive demand were disregarded in Ref. [8].

1.3. Contributions

In this paper, optimal nodal hourly pricing is implemented in a reconfigurable SDN with variable renewable generation and responsive demand. A wind farm as an intermittent renewable energy source and a micro turbine as a dispatchable DG unit are located in the SDN. The SDN benefits from battery energy storage (BES) and is operated by a DisCo. The main contribution of this work is to propose a new two-stage scheduling framework to maximize the profit of the DisCo. In the first stage the proposed framework finds optimal retail electricity prices, while the best network topology and the bidding strategy of the DisCo in the DA energy market are determined in the second stage. The two point estimate method (TPEM) is also implemented in this paper to model the intrinsic uncertainty of wind farm power generation and responsive demand.

1.4. Paper organization

The rest of this paper is organized as follows. The proposed probabilistic optimization framework as well as problem formulation are provided in Section 2. Section 3 presents the two-stage solution procedure. Numerical studies and simulation results along with some observations and discussions are included in section 4, and finally section 5 concludes the paper. The introduction contains a review of literature on the topic.

2. Probabilistic operation scheduling framework

In order to study the effects of topology reconfiguration on the operation scheduling of a SDN with variable renewable power generation and responsive demand, a two-stage probabilistic framework is presented in this section. The SDN contains a wind farm as stochastic renewable and a micro turbine as dispatchable DG and is operated by a DisCo with a natural monopoly. The wind farm and micro turbine are assumed to be investor-owned and send their bids to the DisCo via a communication system. In addition, the DisCo is assumed to be a price taker and bids in the wholesale market for energy sale/purchase at forecasted DA wholesale prices. The main point of connection of the SDN to the upstream network/wholesale market is a distribution substation transformer at the grid supply point. Responsive consumers in the SDN schedule their consumption in response to retail prices using an energy management system. Initial DA demand and DA generation of the wind farm is estimated by the DisCo based on weather forecasts and historical data, which lies outside of the scope of this study. Moreover, the DisCo receives BES and network data as well as estimated DA wholesale market prices via a smart communication system. Network data include the status of RCSs, scheduled feeder outages, and possible network configurations as well as distribution lines data. Input and output data as well as stages of the proposed scheduling framework are shown in Fig. 2. In the first stage, the proposed framework uses input data to determine optimal retail prices based on loads specifications. Other outputs, like the bidding strategy, are omitted at this stage. These optimal retail prices are supposed to be different at each node in each hour and are set to modify the consumption pattern of responsive loads in a way that reduces the energy supply cost of the DisCo while preserving the benefits of consumers. These optimal prices along with other input data are fed to the second stage, which determines the best hourly configuration and the bidding strategy of the DisCo in the DA wholesale market. In order to model the uncertain nature of wind power and responsive demand, the two-point estimate method (TPEM) is applied to the framework. The general formulation of the optimization problem is presented as follows.

2.1. Objective function

The objective function is the DisCo's profit, defined as the difference between revenue and cost. The revenue function includes the income from selling power to the wholesale market and consumers. The sign of $\Pi^t_{UN,i}$ reflects the sell/purchase status of power in time interval t. A negative sign shows that the DisCo purchases power from the wholesale market, while a positive sign reflects selling power to the wholesale market. The cost function consists of BES operation cost, the cost of power purchase from DG units and the DA wholesale market, and eventually the switching cost of RCSs. The operational cost of BES is generally associated with its maintenance costs, and is assumed as a linear function of the absolute of its charged or discharged power at each hour, i.e. $COST^t_{BES,i} = A_{BES,i} \times \Pi^t_{BES,i} + B_{BES,i}$ in which $A_{BES,i}$ and $B_{BES,i}$ are positive. Objective function (expected profit), expected revenue and expected cost are presented in (1), (2) and (3), respectively.

$$\max_{\substack{\lambda^t_{D,i},\ \Pi^t_{DG,i},\ \Pi^t_{BES,i,Ch},\ \Pi^t_{BES,i,Dch},\\ \Pi^t_{UN,i},\ L^t_{DG,i},\ L^t_{BES,Ch},\ L^t_{BES,Dch}}} P = R - \mathrm{C} \tag{1}$$

$$\mathrm{R} = \sum_t \left(\sum_i \left(\Pi^t_{D,i} . \lambda^t_{D,i} \right) + \Pi^t_{UN,i} . \lambda^t_M \right) (2) \tag{2}$$

$$\mathrm{C} = \sum_t \left(\begin{array}{c} \sum_{DG} \left(B_{DG,i} . \Pi^t_{DG,i} . L^t_{DG,i} \right) + \\ \sum_{SDG} \left(B_{SDG,i} . \Pi^t_{SDG,i} \right) + COST^t_{BES,i} \end{array} \right) + COST_{Sw} \tag{3}$$

in which the switching cost ($COST_{Sw}$) is calculated as the summation of hourly switching operation costs needed for DA optimal topology reconfiguration.

2.2. Constraints

Four groups of constraints must be satisfied in the optimization process. The first group includes model and welfare constraints of responsive load. The second one includes technical constraints of the distribution network and AC power flow. The third group includes security and adequacy constraints. The last one contains constraints of dispatchable DGs and also characteristics and constraints of BES.

2.2.1. Model and welfare constraints of responsive load

Responsive consumers in the SDN participate in DRPs to reduce their electricity bills by adjusting their power consumption. A comprehensive model of responsive demand is derived in Ref. [4] based on price elasticity of demand as follows.

$$\prod^t_{D,i} = \prod^t_{D0\,i} \left\{ \begin{array}{c} 1 + \frac{e^t_{D,i} \cdot \left[\lambda^t_{D,i} - \lambda_{D0} \right]}{\lambda_{D0}} \\ + \sum_{\substack{h=1 \\ h \neq t}} e^{t,h}_{D,i} \frac{\left[\lambda^h_{D,i} - \lambda_{D0} \right]}{\lambda_{D0}} \end{array} \right\} \tag{4}$$

Although demand responds to price signals based on the model presented in (4), this response is limited by realistic considerations. Moreover, in order for retail prices to be fair towards both consumers and the DisCo, regulatory bodies impose some regulatory restrictions.

Minimum and maximum demand limits. The minimum and maximum consumption of Dth aggregated load in each time interval can be presented as:

$$\prod^t_{D,i,min} \leq \prod^t_{D\,i} \leq \prod^t_{D,i,max} \tag{5}$$

Minimum energy consumption. Equation (6) represents minimum daily energy consumption required by each consumer:

$$\sum_{t=1}^{24} E^t_{D,i} \geq E^{day}_{D,i,min} \tag{6}$$

Retail price cap. In order to protect consumers against high retail prices, a maximum limitation has to be considered as:

$$\lambda^t_{D,i} \leq \lambda^t_{max} \tag{7}$$

Limit on revenue from each consumer. To encourage consumers to participate in the program, the maximum bill of each consumer is set to be less than if DA wholesale prices were directly sent to consumers. Although retail prices were capped by (7), constraint (8) protects consumers against being offered relatively high prices at most hours of day by the DisCo, aiming to increase the DisCo's benefit. If β (payment factor) is selected less or equal to 1 in (8), the benefits of the DisCo and the consumers who participated in the program are simultaneously derived.
(8)

$$\sum_{t=1}^{24} \prod^t_{D,i} \lambda^t_{D,i} \leq \beta \cdot \sum_{t=1}^{24} \prod^t_{DM,i} \lambda^t_M \tag{8}$$

2.2.2. Network constraints

Power flow equations:.

$$\begin{array}{l} \Pi^t_{G,i} - \Pi^t_{D,i} = \\ \sum_j \left| V^t_i \right| \left| V^t_j \right| \left| Y^t_{ij} \right| \cos \left(\theta_{ij} + \delta^t_j - \delta^t_i \right) \end{array} \tag{9}$$

$$\begin{array}{l} \Psi^t_{G,i} - \Psi^t_{D,i} = \\ \sum_j \left| V^t_i \right| \left| V^t_j \right| \left| Y^t_{ij} \right| \sin \left(\theta_{ij} + \delta^t_j - \delta^t_i \right) \end{array} \tag{10}$$

where $\Pi^t_{G,i}$ and $\Psi^t_{G,i}$ are calculated as follow.

$$\begin{array}{l} \Pi^t_{G,i} = \Pi^t_{DG,i} + \Pi^t_{SDG,i} - \Pi^t_{UN,i} \\ + \eta_{Dch} . \Pi^t_{BES,i,Dch} - \Pi^t_{BES,i,Ch} \end{array} \tag{11}$$

$$\Psi^t_{G,i} = \Psi^t_{UN,i} + \Psi^t_{DG,i} \tag{12}$$

Bus voltage limit:.

$$V^{min}_i \leq V^t_i \leq V^{max}_i \tag{13}$$

Substation capacity limit:.

$$S^t_{UN} \leq S^{max}_{UN} \tag{14}$$

Feeder flow limits:.

$$S^t_{ij} \leq S^{max}_{ij} \tag{15}$$

2.2.3. Adequacy and security constraints

Supply-demand balancing constraints:.

$$\begin{array}{l} \sum_{DG} \Pi^t_{DG,i} + \sum_{SDG} \Pi^t_{SDG,i} + \eta_{Dch} . \Pi^t_{BES,i,Dch} \\ - \Pi^t_{UN,i} = \sum_D \Pi^t_{D,i} + \Pi^t_{Loss} + \Pi^t_{BES,i,Ch} \end{array} \tag{16}$$

$$\Psi^t_{UN,i} + \sum_{DG} \Psi^t_{DG,i} = \sum_D \Psi^t_{D,i} + \Psi^t_{Loss} \tag{17}$$

Reserve capacity:. Due to possible variations in wind farm power generation and responsive demand, this is necessary to ensure that enough capacity exists to meet the hourly demand as well as maintaining a reserve margin. Thus, (γ%) (e.g. 5% based on data given in table 4 of wind farm power generation and (χ%) (e.g. 2% based on information given in [7] about deviation in load demand forecast) of total hourly demand is considered by DisCo as the reserve margin provided by dispatchable DGs as follows.

$$\begin{aligned}&\textstyle\sum_{DG}(\Pi^t_{DG,i,\max} - \Pi^t_{DG,i}) + \Pi^t_{UN,i,\max} + \\ &\Pi^t_{UN,i,B} \geq \chi \textstyle\sum_{SDG} \Pi^t_{SDG,i,B} + \gamma \textstyle\sum_D \Pi^t_{D,i}\end{aligned} \tag{18}$$

where $\Pi^t_{UN,i,\max}$is calculated as follows:

$$\Pi^t_{UN,i,\max} = \sqrt{(S^{max}_{UN,i})^2 - (\Psi^t_{UN,i})^2} \tag{19}$$

2.2.4. Constraints of DGs and BES

Dispatchable DGs constraints:. These constraints are considered to guarantee that the commitment of dispatchable DG units respects the physical limitations of these units. Constraints (20)–(21) are considered to guarantee that the power generated by DG units adhere to the respective capacity limits, minimum up/down times, and ramp rates respectively.

$$\begin{aligned}\Pi^t_{DG,i} &\leq \Pi^t_{DG,i,\max}.L^t_{DG,i}\\ \Pi^t_{DG,i} &\geq \Pi^t_{DG,i,\min}.L^t_{DG,i}\end{aligned} \tag{20}$$

$$\begin{cases}\sum_{h=1}^{MUT} L^{t+h-1}_{DG,i} \geq MUP_{DG,i} \ \ \forall\, M^t_{DG,i} = 1\\ \sum_{h=1}^{MDT} (1 - L^{t+h-1}_{DG,i}) \geq MDT_{DG,i} \ \forall\, N^t_{DG,i} = 1\\ M^t_{DG,i} - N^t_{DG,i} = L^t_{DG,i} - L^{t-1}_{DG,i}\\ M^t_{DG,i} + N^t_{DG,i} \leq 1\end{cases} \tag{21}$$

$$\begin{aligned}\Pi^{t+1}_{DG,i} - \Pi^t_{DG,i} &\leq RUP_{DG,i}\\ \Pi^t_{DG,i} - \Pi^{t+1}_{DG,i} &\leq RDN_{DG,i}\end{aligned} \tag{22}$$

BES characteristics and constraints:. The maximum charge/discharge rate of a BES is limited by constraints (23) and (24) respectively.

$$0 =\leq \prod^{t}_{BES,i,Ch} \leq \prod^{max}_{BES,Ch} \cdot L^t_{BES,Ch} \tag{23}$$

$$0 =\leq \prod^{t}_{BES,i,Dch} \leq \prod^{max}_{BES,Dch} \cdot L^t_{BES,Dch} \tag{24}$$

Constraint (25) ensures that the relationship between charge/discharge binary variables are logical.

$$L^t_{BES,Ch} + L^t_{BES,Dch} \leq 1 the \tag{25}$$

Equation (26) models the stored energy in a BES while constraint (27) ensures that this energy is within the upper and lower capacity limits of the BES.

$$\begin{aligned}&E^t_{BES,i} = E^{t-1}_{BES,i} + \\ &\eta_{Ch} \times \Pi^t_{BES,i,Ch} - \Pi^t_{BES,i,Dch}\end{aligned} \tag{26}$$

$$E^{min}_{BEs} \leq E^t_{BES,i} \leq E^{max}_{BES} \tag{27}$$

2.3. Uncertainty modeling of wind power and responsive demand

The TPEM is known as an efficient means of handling uncertainties with an acceptable level of simplicity and accuracy [21]. This approach only requires solving 2×m scenarios to obtain the behavior of m random variables [12]. Stochastic variables here are initial hourly demand and wind farm power generation assumed as uncorrelated variables. These stochastic variables are modeled as zero-mean normally-distributed random variables with a standard deviation of σ [12].

In order to model the behavior of m random variables by using the TPEM, suppose $P : \{p_1, p_2, ..., p_l, ..., p_m\}$ is a random variable with a mean value μ and standard deviationσ. Z is a random quantity in function of P: Z = F(P). Each of the k concentrations of the random variables$p_l$is defined as a pair composed of a location$p_{l,k}$and a weight$w_{l,k}$. The location is determined as follows.

$$p_{l,k} = \mu_{p_l} + \xi_{l,k}\sigma_{p_l} \tag{28}$$

where $\xi_{l,k}$ is the standard location of p_l. The standard locations and weights are computed as:

$$\begin{aligned}\xi_{l,1} &= \tfrac{\lambda_{l,3}}{2} + \sqrt{m + \left(\tfrac{\lambda_{l,3}}{2}\right)^2}\\ \xi_{l,2} &= \tfrac{\lambda_{l,3}}{2} - \sqrt{m + \left(\tfrac{\lambda_{l,3}}{2}\right)^2}\end{aligned} \tag{29}$$

and

$$\begin{aligned}w_{l,1} &= -\tfrac{1}{m}\tfrac{\xi_{l,2}}{\xi_{l,1}-\xi_{l,2}}\\ w_{l,2} &= \tfrac{1}{m}\tfrac{\xi_{l,1}}{\xi_{l,1}-\xi_{l,2}}\end{aligned} \tag{30}$$

where $\lambda_{l,3}$ denotes the skewness of:

$$\lambda_{l,3} = \frac{E\left[\left(p_l - \mu_{p_l}\right)^3\right]}{\left(\sigma_{p_l}\right)^3} \tag{31}$$

In each time, one of the variables concentrations with the means of other variables is taken into account and eventually the statistical information of the output variable are computed.

$$Z_{l,k} = F\left(p_{l,1},\ p_{l,2}, ...,\ p_{l,k}, ...,\ p_{m,k}\right) \tag{32}$$

$$E\left(Z\right) \cong E\left(Z\right) + \sum_k w_{l,k} \cdot Z_{l,k} \tag{33}$$

The detailed procedure of the TPEM discussed in Ref. [21] is illustrated in Fig. 1.

2.4. The solution method

2.4.1. First stage: Nodal hourly pricing

In the above section the proposed probabilistic optimization framework is formulated as a MINLP problem. In the first stage retail hourly prices are calculated as a part of the objective function with the aim of maximizing the DisCo's profit. These prices are not the same for all consumers and are

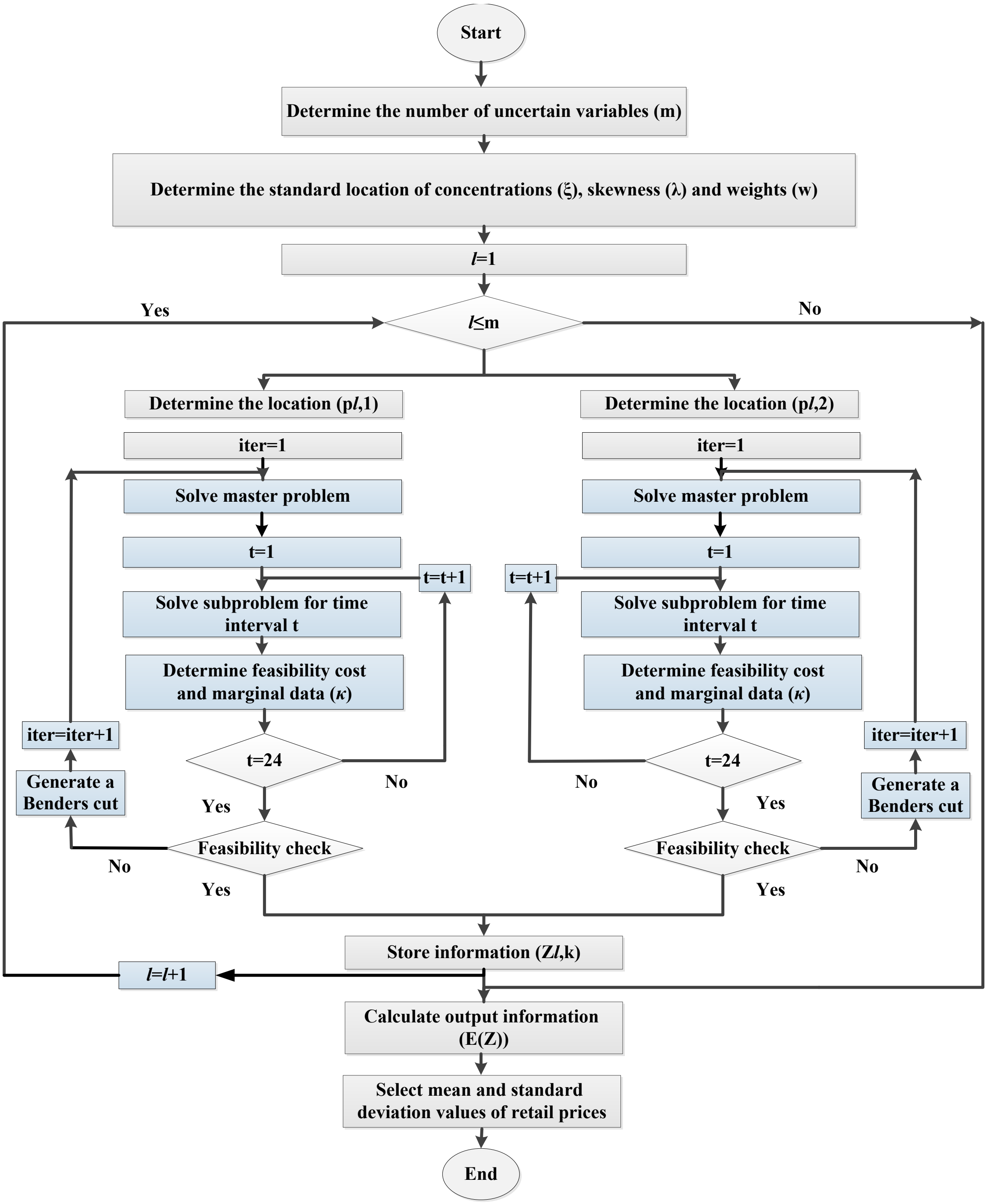

Figure 1: Flowchart of the solution method

determined based on load specifications. Although network configuration is supposed to be fixed in this stage, difficulties associated with solving the proposed MINLP problem in a real size distribution system makes it inevitable to apply decomposition algorithms, such as the BDT [16, 19]. This technique partitions the problem into two levels, including a master and slave problem. Then it utilizes an iterative procedure between these levels, aiming to find an optimal solution [19]. The master problem determines retail prices, disregarding network constraints, whereas the slave problem deals with network constraints. Other master problem solutions including BES charge/discharge power, dispatchable DGs power generation and power exchange with upstream network are transferred to the slave problem. The constraints of the slave problem check the feasibility of the master problem solutions and return marginal data and dual values of these variables to the master problem to be used in Benders cuts. Benders cuts, master problem solutions and slave problem marginal data are updated in each iteration. The iterative procedure continues until marginal data go to zero and all hourly variables reach their optimal value. The objective function value in this condition is maximum profit of the DisCo. This iterative procedure is illustrated in Fig. 1 and details are discussed as follows.

Master problem . The master problem objective function is formulated as follows.

$$\max_{\substack{\lambda^t_{D,i},\Pi^t_{DG,i},\Pi^t_{BES,i,Ch},\Pi^t_{BES,i,Dch},\\ \Pi^t_{UN,i},L^t_{DG,i},L^t_{BES,Ch},L^t_{BES,Dch}}} \quad \mathrm{P}-\sum_t \alpha^t_{Sco} \tag{34}$$

Subject to constraints 5-8, 11-12, 14-27 and the Benders cuts:

$$\begin{aligned}&\alpha^t_{Sco} \geq \alpha^t_{n-1}+\\ &\textstyle\sum_D \kappa^t_{D,i,n-1}\left(\Pi^t_{D,i}-\overline{\Pi}^t_{D,i,n-1}\right)+\\ &\textstyle\sum_{DG} \kappa^t_{DG,i,n-1}\left(\Pi^t_{DG,i}-\overline{\Pi}^t_{DG,i,n-1}\right)\\ &+\kappa^t_{UN,i,n-1}\left(\Pi^t_{UN,i}-\overline{\Pi}^t_{UN,i,n-1}\right)+\\ &\kappa^t_{BES,Ch,n-1}\left(\Pi^t_{BES,Ch,i}-\overline{\Pi}^t_{BES,Ch,i,n-1}\right)\\ &+\kappa^t_{BES,Dch,n-1}\left(\Pi^t_{BES,Ch,i}-\overline{\Pi}^t_{BES,Ch,i,n-1}\right)\end{aligned} \tag{35}$$

where α^t_{Sco} is the subproblem cost and $\overline{\Pi}^t_{D,i,n-1}$, $\overline{\Pi}^t_{DG,i,n-1}$, $\overline{\Pi}^t_{UN,i,n-1}$, $\overline{\Pi}^t_{BES,i,Ch,n-1}$ and $\overline{\Pi}^t_{BES,i,Dch,n-1}$are solutions of subproblem at iteration n-1. The first and second terms of (34) represent the DisCo's profit and feasibility costs of each hourly subproblem respectively.

Subproblem . The subproblem checks the feasibility of the master problem solutions using AC power flow. The objective function presented in (36) minimizes the cost of deviations from the master problem solutions in each time interval:

$$\begin{aligned}&\min_{\Pi^t_{D,i},\Pi^t_{DG,i},\Pi^t_{BES,i,Ch},\Pi^t_{BES,i,Dch},\Pi^t_{UN,i}}\\ &\textstyle\sum_i r^t_{\Pi,UP,i}+r^t_{\Pi,DN,i}+r^t_{\Psi,UP,i}+r^t_{\Psi,UP,i}\end{aligned} \tag{36}$$

where$r^t_{\Pi,UP,i}$, $r^t_{\Pi,DN,i}$, $r^t_{\Psi,UP,i}$ and $r^t_{\Psi,UP,i}$ are slack variables of the optimization problem added to AC power flow equations to make the subproblem feasible. Subproblem constraints including (37)–(39) check the feasibility of the master problem solutions in all hours and generate marginal data and dual values. These values update Benders cuts in each iteration which in turn improves master problem solutions. This iterative procedure goes on until the master problem solution is feasible.

$$\begin{aligned}&\Pi^t_{G,i}-\Pi^t_{D,i}+r^t_{\Pi,UP,i}-r^t_{\Pi,DN,i}=\\ &\textstyle\sum_j \left|V^t_i\right|\left|V^t_j\right|\left|Y^t_{ij}\right|\cos\left(\theta_{ij}+\delta^t_j-\delta^t_i\right)\end{aligned} \tag{37}$$

$$\begin{aligned}&\Psi^t_{G,i}-\Psi^t_{D,i}+r^t_{\Psi,UP,i}-r^t_{\Psi,DN,i}=\\ &\textstyle\sum_j \left|V^t_i\right|\left|V^t_j\right|\left|Y^t_{ij}\right|\sin\left(\theta_{ij}+\delta^t_j-\delta^t_i\right)\end{aligned} \tag{38}$$

$$\begin{aligned}&\Pi^t_{D,i}=\overline{\Pi}^t_{D,i}\leftrightarrow\kappa^t_{D,i,n-1};\\ &\Pi^t_{DG,i}=\overline{\Pi}^t_{DG,i}\leftrightarrow\kappa^t_{DG,i,n-1};\\ &\Pi^t_{UN,i}=\overline{\Pi}^t_{UN,i}\leftrightarrow\kappa^t_{UN,i,n-1};\\ &\Pi^t_{BES,Ch,i}=\overline{\Pi}^t_{BES,Ch,i}\leftrightarrow\kappa^t_{BES,Ch,i,n-1};\\ &\Pi^t_{BES,Dch,i}=\overline{\Pi}^t_{BES,Dch,i}\leftrightarrow\kappa^t_{BES,Dch,i,n-1}\end{aligned} \tag{39}$$

where$\overline{\Pi}^t_{D,i}$, $\overline{\Pi}^t_{UN,i}$, $\overline{\Pi}^t_{DG,i}$, $\overline{\Pi}^t_{BES,Ch,i}$and $\overline{\Pi}^t_{BES,Dch,i}$are the results of the master problem at the same iteration and $\kappa^t_{D,i,n-1}$, $\kappa^t_{UN,i,n-1}$, $\kappa^t_{DG,i,n-1}$, $\kappa^t_{BES,Ch,i,n-1}$ and $\kappa^t_{BES,Dch,i,n-1}$are dual variables associated with these optimal solution.

The optimization problem is implemented in GAMS software, and SBB and CONOPT solvers are selected to solve master and slave problems respectively [1]. The average simulation time of the first stage is 10.02 seconds.

2.4.2. Second stage: Topology reconfiguration

The main objective of the optimization model in the second stage is to find the best topology configuration among different possible configurations in each hour. Optimal retail prices determined in the first stage in addition to other input data shown in Fig. 2 are fed to the second stage. Equations (40)–(42) are used in the second stage to model and optimize DA DisCo operation. In order to choose the best network topology in each hour, equations (40)–(42) are also implemented in the model. In these equations a binary variable (LL^t_{ii}) as well as line data (Y, θ) are attributed to each topology. When a topology binary variable is set to 1 by the optimization program for each hour, the related SDN configuration is used for power flow calculations and checking constraints.

$$Y=Y_1LL^t_1+Y_2LL^t_2+Y_3LL^t_3 \tag{40}$$

$$\theta=\theta_1LL^t_1+\theta_2LL^t_2+\theta_3LL^t_3 \tag{41}$$

$$LL^t_1+LL^t_2+LL^t_3=1 \tag{42}$$

The optimization model in the second stage formulated as a MINLP problem is implemented in GAMS software and SBB solver is selected to solve it [1]. The average simulation time of the second stage is 16.52 seconds.

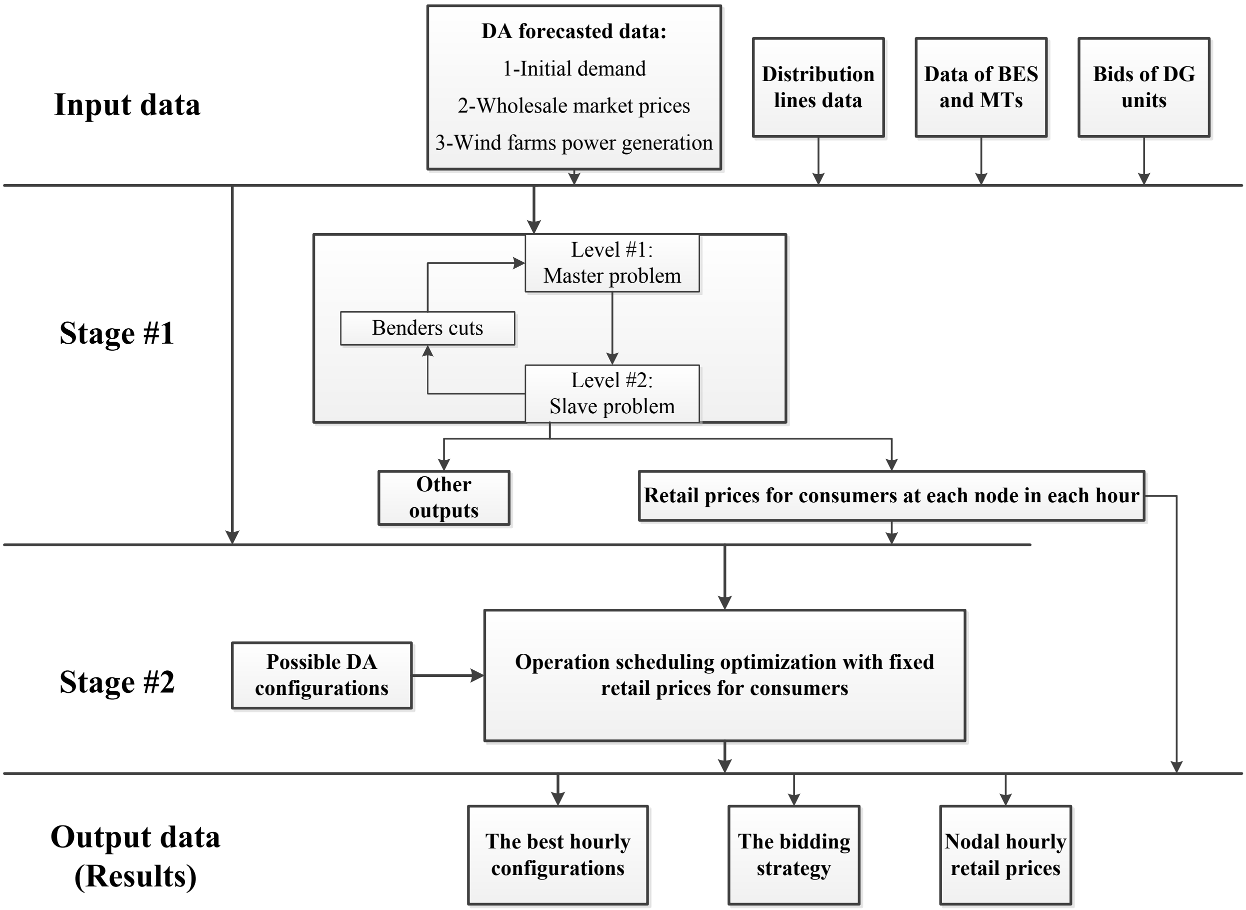

Figure 2: The proposed operation scheduling framework for a reconfigurable SDN

Table 1: Characteristics of the stochastic DG

DG no	Bus no	$\prod_{SGD,i}^{min}$, MW	$\prod_{SGD,i}^{max}$, MW	$B_{SDG,i}$, \$/MWh
1	14	0	11	48

Table 2: Characteristics of the BES

Capacity, MWh	$\prod_{Ch}^{max}$, MW	$\prod_{Dch}^{max}$, MW	η_{Ch}, η_{Dch}	Initial level, MWh	A_{Ch}, A_{Dch}, \$	B_{Ch}, B_{Dch}, \$	C, \$
9	1.2	1.2	0.9	2	11	9	3

3. Numerical studies

3.1. Data and required assumptions

In this section the proposed optimization framework is implemented on an 18-buses distribution network. The base topology shown in Figs 3–5 a was extracted from the IEEE-30 buses system by considering only the 33 kV networks [3]. In addition, two other topologies considered in this work were constructed considering the base topology and are shown in Figs 4 and 5. The DisCo operates a BES located at bus 7, and the network is connected to the upstream network at bus 1 through a substation transformer. The cost function coefficients and other BES data are given in Table 2 and the substation transformer capacity at bus 1 is assumed at 50 MVA. Furthermore, a wind farm as stochastic DG is located at bus 14 while a micro turbine is considered as a dispatchable DG unit at bus 11. The bid price of each DG is set based on its levelized cost of electricity (LCOE). The LCOE is evaluated on the basis of the capital cost, time of operation, maintenance and operation cost and lifetime of the DG [3]. Moreover, the LCOE should take into account additional costs of communication and control infrastructures installed to coordinate the operation of different DGs in the DisCo. Dispatchable DG data as well as Stochastic DG data and its forecast power generation are presented in Tables 3–4 respectively.

Three types of consumers—residential, commercial and small industrial consumers—are connected to the system buses. The consumers at each bus are assumed to be the same type and are modeled as a single lumped load. Self- and cross-price elasticities for all load types are shown in Table 5, which is compatible with Ref. [4]. It should be noted that a precise estimation of elasticity coefficients requires a complex econometric procedure, which is not in the scope of this paper. Table 6 presents different time intervals considered in this work. Fig. 6 shows DA hourly electricity prices on a typical day (February 18 2014) obtained from the wholesale electricity market data of Ontario, Canada [2]. The base energy price is assumed as (101\$/MWh) in all numerical studies, which is the average of wholesale market prices during February 2014 [2]. Moreover, this price (101\$/MWh) is also assumed as the electricity rate in flat pricing. The mean value of initial demand in each hour is given in Fig. 7. The standard deviation of initial demand in each hour is supposed to be 3% of its mean value. Furthermore, the maximum and minimum limits for elastic load demand are equal to 130% and 70% of the initial demand forecast, respectively. In addition, the minimum daily energy consumption of each elastic load is assumed as 90% of its initial consumption and the payment factor (β) is assumed to be 1.

Table 4: DA generation forecast of the stochastic DG

Hour	SDG1 (BUS 14), MW	
	Mean	St. De
t=1, ..., 6	4	0.1
t=7, ..., 12	5	0.3
t=13, ..., 18	9	0.4

Table 5: Self- and cross-elasticities

Bus no	Load Type	Self Elasticity	Cross Elasticity
2, 3, 4, 5	Residential	-0.01	0.001
8, 9	Commercial	-0.025	0.0025
6	Industrial	-0.04	0.004
13	Industrial	-0.05	0.005
15	Industrial	-0.07	0.007

3.2. Case study and discussion

In this section the proposed framework was applied to optimize the operation scheduling of a SDN with reconfigurable topology. In addition, the TPEM was implemented to the optimization model in order to consider the uncertainty associated with wind farm power generation and initial demand. Therefore, all results are probabilistic in nature and are presented in the form of mean values. Moreover, the most repeated topology for each hour was determined as a suggestion for the next day. The best SDN topology for each hour determined by the optimization framework is presented

Table 3: Characteristics of the dispatchable DG

DG no	Bus no	$\prod_{GD,i}^{min}$, MW	$\prod_{GD,i}^{max}$, MW	$B_{SDG,i}$, \$/MWh	$SUP_{DG,i}$, \$	$SDN_{DG,i}$, \$
1	11	1	5	108	5	3

Table 6: Time intervals

Time intervals	Hours
Off-peak	22–24 and 1–6
Mid-peak	11–16
On-peak	7–10 and 17–21

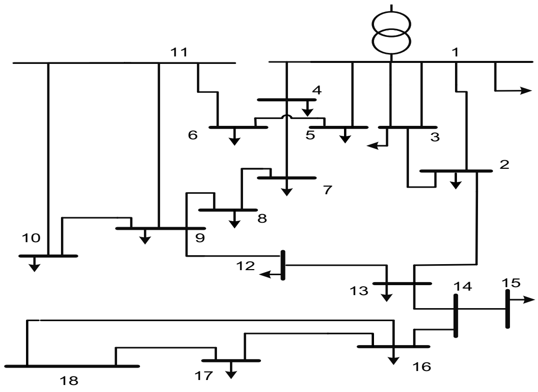

Figure 3: The 18-bus distribution system. Topology T_1 (The base topology)

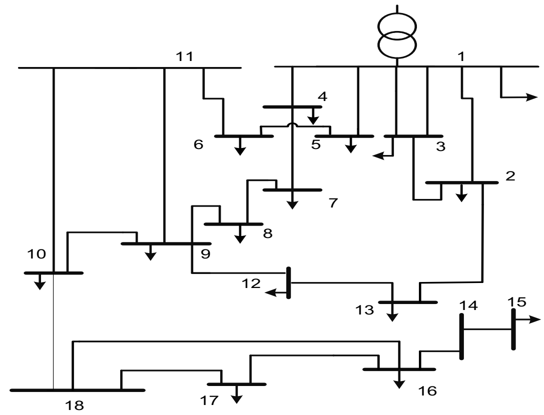

Figure 5: The 18-bus distribution system. Topology T_3

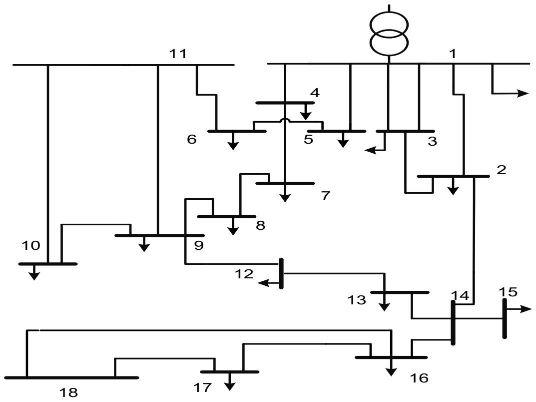

Figure 4: The 18-bus distribution system. Topology T_2

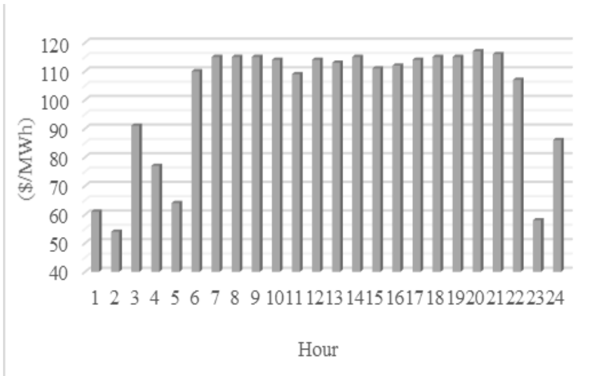

Figure 6: DA forecasted wholesale market prices

in Table 7. Topology T_2 was the one most often selected by the framework during hours with high wind power generation. This is due to the fact that in this topology the line 2-14 facilitates grid integration of the wind farm at bus 11. During hours with lower wind power penetration, topologies $T_1$and T_3 were selected.

Optimal scheduling of the dispatchable DG unit is presented in Fig. 8. DG1 is "OFF" during hours 1-5 and 22-24 because wholesale market prices in these hours are lower than the production cost of this unit. In fact, because of the capability of DisCo to sell power to the wholesale market, the generation pattern of DG units does not depend on the demand profile but is determined based only on DA wholesale market prices. The amount of power exchange with the wholesale market in each hour is presented in Fig. 9. The DisCo purchases power from the wholesale market during hours 7-12 and 19 to meet its demand. Moreover, the DisCo prefers to purchase power from the wholesale market during low-price hours, like 1-6 and 22-24. In contrast the DisCo sells its surplus power to the wholesale market during high-price hours, like 13-17 and 20-21, to increase its profit. As seen from Fig. 10, the BES is charged during hours 1-2 when wholesale market prices are low and is discharged during hours 20-21 when wholesale market prices are at the highest values.

In order to show the effectiveness of optimal topology reconfiguration, the results are compared with the case of fixed topology configuration from the technical and economic points of view. Technical criteria including total line loss and total voltage deviation $(\sum_i \sum_t |v(i, t) - 1|)$ in systems' buses as well as the economic criterion (DisCo's profit) are given in Table 8. As can be observed, topology reconfiguration reduces total voltage deviation and total line losses, while the DisCo's profit is increased when optimal topology reconfiguration is implemented in the network.

4. Conclusion

In this paper, a new two-stage operation scheduling framework is presented to determine the best network topology for a reconfigurable SDN in each hour. The SDN contains uncertain renewable generation as well as responsive demand, and is operated by a DisCo. Retail hourly prices for responsive consumers are determined in the first stage of the proposed framework. The second stage determines the best network topology and the bidding strategy of the DisCo in the DA energy market. Moreover, the TPEM is applied to the framework to model the uncertainty associated with wind

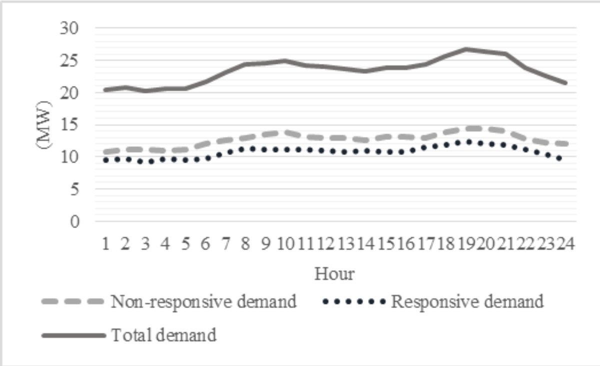

Figure 7: DA demand profile

power generation and responsive demand. The effectiveness of the proposed scheduling framework has been validated through numerical studies. The results confirm that the implementation of network topology reconfiguration in addition to price-based DRP improves technical and economic criteria of SDN operation.

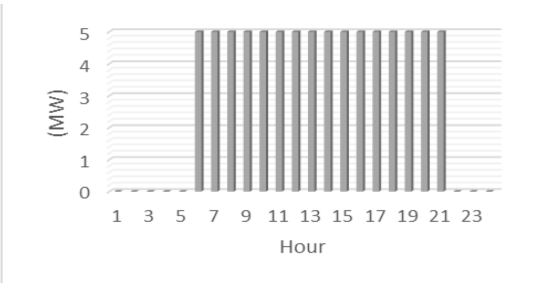

Figure 8: Optimal dispatch of DG1

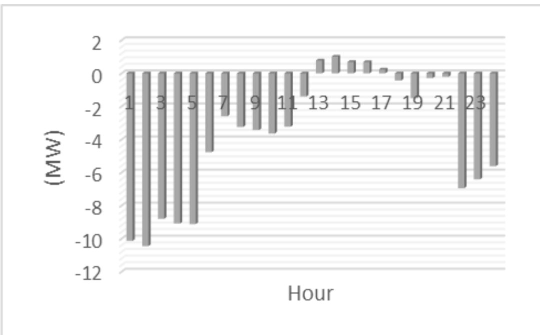

Figure 9: Hourly power exchange with the wholesale energy market

Table 7: The best topology for each hour

Hour	Topology
1	T_3
2	T_1
3	T_1
4	T_3
5	T_3
6	T_1
7	T_1
8	T_1
9	T_1
10	T_1
11	T_2
12	T_2
13	T_2
14	T_2
15	T_2
16	T_2
17	T_2
18	T_2
19	T_2
20	T_2
21	T_2
22	T_2
23	T_2
24	T_2

Table 8: Economic and technical criteria

	Profit, $	Total loss, MW	Total voltage deviation, PU
Fixed topology	9438.041	1.357	1.103
Reconfigurable topology	9467.064	1.117	0.8267

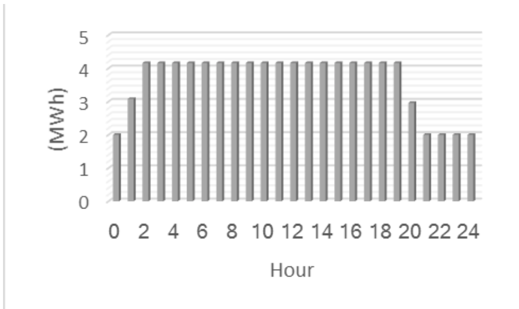

Figure 10: The BES level in each hour

References

[1] Gams webpage. URL `http://www.gams.com`.

[2] Ontario energy board (oeb). regulated price plan manual. URL `http://www.ontarioenergyboard.ca/OEB/Documents/EB-2004-0205/RPP-Manual pdf`.

[3] http://www.ee.washington.edu/research/pstca/pf30/pg_tca30bus.html.

[4] H. A. Aalami, M. ParsaMoghaddam, and G. R. Yousefi. Demand response modeling considering interruptible/curtailable loads and capacity market programs. *Applied Ener*, 87:243–250, 2010.

[5] G. Angevine and D. Hrytzak-Lieffers. Ontario industrial electricity demand responsiveness to price. The Fraser Institute, 2007.

[6] M. Doostizadeh and H. Ghasemi. A day-ahead electricity pricing model based on smart metering and demand-side management. *Energy*, 46: 221–230, 2012.

[7] FERC. Staff report.: Assessment of demand response and advanced metering. URL `http://www.FERC.gov`.

[8] A. Ghasemi, S. S. Mortazavi, and E. Mashhour. Integration of nodal hourly pricing in day-ahead sdc (smart distribution company) optimization framework to effectively activate demand response. *Energy*, 86:

649–660, 2015.

[9] S. Golshannavaz, S. Afsharnia, and F. Aminifar. Smart distribution grid: Optimal day-ahead scheduling with reconfigurable topology. *IEEE Transactions on Smart Grid*, 5(5):2402–2411, 2014.

[10] R. Jabbari-Sabet, S. M. Moghaddas-Tafreshi, and S. S. Mirhoseini. Microgrid operation and management using probabilistic reconfiguration and unit commitment. *International Journal of Electrical Power & Energy Systems*, 75:328–336, 2016.

[11] A. Kumar, S. C. Srivastava, and S. N. Singh. A zonal congestion management approach using real and reactive power rescheduling. *IEEE Transactions on Power Systems*, 19(1):554–562, 2004.

[12] M. Moeini-Aghtaie, A. Abbaspour, and M. Fotuhi-Firuzabad. Incorporating large-scale distant wind farms in probabilistic transmission expansion planning—part i: Theory and algorithm. *IEEE Transactions on Power Systems*, 27(3):1585–1593, 2012.

[13] B. Moradzadeh and K. Tomsovic. Mixed integer programming-based reconfiguration of a distribution system with battery storage. In *Proceedings of North American Power Symposium*, Champaign, IL, USA, sep 2012.

[14] L. Nikonowicz and J. Milewski. Virtual power plants - general review: structure, application and optimization. *Journal of Power Technologies*, 92(3):135–149, 2012.

[15] M. Parastegari, R. A. Hooshmand, A. Khodabakhshian, and A. H. Zare. Joint operation of wind farm, photovoltaic, pump-storage and energy storage devices in energy and reserve markets. *International Journal of Electrical Power & Energy Systems*, 64:275–284, 2015.

[16] S. Rahimi, Niknam T., and F. Fallahi. A new approach based on benders decomposition for unit commitment problem. *World Applied Science Journal*, 6(12):1665–1672, 2009.

[17] A. Safdarian, M. Fotuhi-Firuzabad, and M. Lehtonen. Integration of price-based demand response in DisCos' short-term decision model. *IEEE Transactions on Smart Grid*, 5(5):2235–2245, 2014.

[18] F. C. Schweppe, M. C. Caramanis, R. D. Tabors, and R. E. Bohn. Spot pricing of electricity, 1989.

[19] M. Shahidehpour and Y. Fu. Benders decomposition: applying benders decomposition to power systems. *IEEE Power and Energy Magazine*, 3(2):1–2, 2005.

[20] T. Sousa, H. Morais, Z. Vale, P. Faria, and J. Soares. Intelligent energy resource management considering vehicle-to-grid: A simulated annealing approach. *IEEE Transactions on Smart Grid*, 3(1):535–542, 2012.

[21] G. Verbic and C. A. Canizares. Probabilistic optimal power flow in electricity markets based on a two-point estimate method. *IEEE Transactions on Power Systems*, 21:1–11, 2006.